Available online at www.sciencedirect.com
SCIENCE DIRECT®
Journal of Colloid and Interface Science 274 (2004) 41–48
JOURNAL OF Colloid and Interface Science
www.elsevier.com/locate/jcis

Synthesis and characterization of tri(ethylene oxide)-attached poly(amidoamine) dendrimer layers on gold

Mi-Young Hong,[a] Young-Ja Kim,[a] Jae Wook Lee,[b,1] Kimoon Kim,[b] Jung-Hwa Lee,[c] Jong-Shin Yoo,[c] Sung-Hun Bae,[d] Byong-Seok Choi,[d] and Hak-Sung Kim [a,*]

[a] *Department of Biological Sciences, Korea Advanced Institute of Science and Technology 373-1, Kusung-dong, Yusung-ku, Taejon 305-701, South Korea*
[b] *National Creative Research Initiative Center for Smart Supramolecules and Department of Chemistry, Division of Molecular and Life Sciences, Pohang University of Science and Technology, San 31 Hyojadong, Pohang 790-784, South Korea*
[c] *Korea Basic Science Institute, Taejon 305-333, South Korea*
[d] *Department of Chemistry, KAIST, Taejon 305-701, South Korea*

Received 6 June 2003; accepted 6 November 2003

Abstract

This paper describes the synthesis of a tri(ethylene oxide)-attached fourth-generation poly(amidoamine) dendrimer (EO_3-dendrimer) and the characterization of its layers on gold. NMR analysis and matrix-assisted laser desorption/ionization time-of-flight mass spectrometry revealed that about 61 amine groups of a G4 PAMAM dendrimer were covalently conjugated with tri(ethylene oxide) units, accounting for a 95% modification level. Layers of the EO_3-dendrimer were formed on gold, and the resulting surface was characterized by infrared reflection absorption spectroscopy, ellipsometry, and contact angle goniometry. The EO_3-dendrimer resulted in more hydrophilic and less compact layers with no substantial deformation of the molecule during layer formation by virtue of the EO_3 units, compared to a PAMAM dendrimer. Interestingly, the specific binding of avidin to the biotinylated layers of the EO_3-dendrimer approached a surface density of 5.2 ± 0.2 ng mm^{-2}, showing about 92% of full surface coverage. The layers of the EO_3-dendrimer were found to be more resistant to nonspecific adsorption of proteins than PAMAM dendrimer layers when bovine serum albumin and serum proteins were tested.

Keywords: Tri(ethylene oxide)-attached dendrimer layer; Biomolecular interface; Nonspecific protein adsorption; Avidin–biotin interaction

1. Introduction

Highly branched dendritic macromolecules (dendrimers) have attracted great attention and been extensively studied due to their unique structural features, such as structural homogeneity, molecular integrity, controlled composition, and multiple chain-ends [1,2]. Relating to dendrimer-based surfaces or interfaces, Crooks and colleagues proposed various techniques and considered their potential for technological applications in construction and characterization of dendrimer monolayers on metal surfaces [3–6]. Other approaches employing dendrimers as building units of nanostructures [7–11] or biosensing devices [12–15] have also been attempted. Recently, we demonstrated that monolayers of a fourth-generation poly(amidoamine) (G4 PAMAM) dendrimer on gold offer some advantages as a biomolecular interface for protein–ligand interactions [16,17]. It was suggested that efficient avidin–biotin interactions at dendrimer monolayers originate from their structural features, such as a corrugated surface and surface exposure of functionalized biotin ligands. Nonspecific adsorption by avidin, onto the dendrimer monolayers, however, was observed to be about 12% relative to the specific avidin binding. This finding might limit the versatile use of the G4 PAMAM dendrimer monolayers as a biomolecular interface.

Besides the necessity of achieving a high density of probes and efficient binding with partners, minimization of nonspecific protein adsorption to improve the selectivity and sensitivity of bioaffinity sensing is also of great significance in biochip-related technologies. A number of strategies have been attempted to minimize nonspecific protein adsorption

* Corresponding author.
E-mail addresses: kkim@postech.ac.kr (K. Kim), hskim76@kaist.ac.kr (H.-S. Kim).
[1] Current address: Department of Chemistry, Dong-A University, Busan 604-714, South Korea.

0021-9797/$ – see front matter © 2004 Published by Elsevier Inc.
doi:10.1016/j.jcis.2003.11.061

on a solid surface [18–23], even though the mechanism of protein adsorption onto a chemically modified surface remains to be elucidated. Widely introduced with a priority, ethylene glycol or ethylene oxide moieties have been recognized for a long time as being able to render surfaces most resistant to protein adsorption, mainly due to steric repulsion and excluded-volume effects [24–26].

In this paper, we describe the synthesis and characterization of tri(ethylene oxide)-attached fourth-generation poly(amidoamine) dendrimer (EO_3-dendrimer) layers on gold. Conjugation of tri(ethylene oxide) units with PAMAM dendrimers was expected to be more effective in reducing nonspecific adsorption of proteins, retaining the unique structural features of the dendrimer molecule. Previously, poly(ethylene glycol)-conjugated PAMAM dendrimers were employed as gene/drug carriers or polymer templates for stabilization of polydisperse nanoparticles [27–30]. We first synthesized the EO_3-dendrimer and constructed its layers on gold. Incorporation of EO_3 units into the dendrimer's chain-ends was confirmed by ^{1}H and ^{13}C NMR spectroscopy and matrix-assisted laser desorption/ionization mass spectrometry (MALDI-TOF MS). The surface properties of the EO_3-dendrimer layers on gold were characterized by various analytical tools. The EO_3-dendrimer layers were also investigated in terms of surface coverage by avidin and nonspecific protein adsorption, using surface plasmon resonance (SPR) spectroscopy and fluorescence microscopy, respectively. Details are reported herein.

2. Experimental

2.1. Chemicals and reagents

Fourth-generation (G4) poly(amidoamine) (PAMAM) dendrimer, 4-nitrophenyl chloroformate, and 11-mercaptoundecanoic acid were purchased from Aldrich. 1-Ethyl-3-(3-dimethylaminopropyl)carbodiimide hydrochloride (EDAC), biotinyl-ε-amidocaproic acid *N*-hydroxysulfosuccinimide ester (sulfo-NHS-biotin), fluorescein isothiocyanate (FITC), FITC-labeled bovine serum albumin (FITC-labeled BSA), and avidin were used as received from Sigma. *N*-hydroxysulfosuccinimide (sulfo-NHS) and human serum were obtained from Pierce. All other reagents and organic solvents used were of the highest quality available and were purchased from the regular source. Doubly distilled and deionized water was used throughout the work. For the buffer solution, phosphate-buffered saline containing 10 mM phosphate, 17 mM KCl, and 138 mM NaCl (PBS, pH 7.4) was used.

2.2. Construction of PAMAM dendrimer and EO_3-dendrimer layers on gold

PAMAM dendrimers and EO_3-dendrimers were covalently attached to reactive SAMs on gold according to the reported procedures [3,16,17]. A freshly evaporated gold surface was prepared by the resistive evaporation of Au (150 nm) onto titanium-primed (20 nm) Si[100] wafers. A gold-coated surface was first cleaned for 5 min with piranha solution (1:4 = 30% H_2O_2:concentrated H_2SO_4 (v/v)). (*Caution: Piranha solution reacts violently with most organic materials and must be handled with extreme care.*) The cleaned surface was chemisorbed with 11-mercaptoundecanoic acids (MUA, 2 mM) in ethanol for 2 h. After cleaning with ethanol and water, the MUA SAM surface was activated with an aliquot containing EDAC (400 mM) and sulfo-NHS (100 mM) for 1 h and then reacted with a methanolic solution of PAMAM dendrimers or an aqueous solution of EO_3-dendrimer (11 mM, based on the primary amine concentration) for 5 h. To hydrolyze the residual esters and detach surface-adsorbed molecules, the dendrimer-layered surface was immersed in an aqueous solution of 10 mM NaOH containing 0.01% Triton X-100 ($\sim$pH 11) for 1 h. After a thorough rinse with distilled water, the dendrimer-modified substrate was stored in PBS buffer until further analysis.

2.3. Surface analysis

Prior to surface characterization, the dendrimer-modified substrates immersed in PBS buffer were rinsed with distilled water and dried with N_2 gas. Infrared reflection–absorption (IR-RA) spectroscopy was conducted in a single reflection mode on a N_2-purged Thermo-Nicolet Nexus FT-IR spectrometer equipped with a Smart SAGA (smart apertured grazing angle) accessory. The *p*-polarized light was reflected off the surface at an 80° angle. An MCT detector cooled with liquid N_2 was used to detect the reflected light with a spectral resolution of 2 cm^{-1}. All spectra were reported in the absorption mode relative to a clean gold surface and spectra analysis was done using standard Nicolet software.

Ellipsometric thickness was determined in air by a Jobin Yvon spectroscopic ellipsometer with a 70° angle of incidence at 632.8 nm wavelength. Film thicknesses of dendrimer layers on a SAM surface were calculated based on a refractive index of 1.46 for dendrimers and *n*-alkanethiols [5]. At least five different locations in each sample were measured and an average value was then calculated.

Contact angles were measured by the sessile drop technique using a DSA 10Mk2 drop shape analysis system at ambient laboratory temperature (20–25 °C). After a 2-μl drop of distilled water was applied to the surface, contact angles were determined within 30 s of the contact. Five different samples were measured and an average value was calculated.

2.4. Avidin–biotin interaction and protein adsorption experiments

To investigate avidin–biotin interaction, EO_3-dendrimer layers were formed on the sensor chip with an evaporated

gold surface (BIAcore) using the same procedures as mentioned earlier. The resulting dendrimer-layered chip was docked into a Biacore-X instrument and functionalized with biotin by running a sulfo-NHS-biotin reagent (2 mg/ml in 0.1 M bicarbonate buffer, pH 9.5) with a flow rate of 3 µl/min for 1 h. After rinsing with PBS buffer, the avidin sample (50 µg/ml in PBS) was injected over the biotinylated surface for 30 min. The avidin-associated surface was washed with an eluent buffer for 10 min, and the SPR angle shift for avidin association was recorded. The nonspecific binding of avidin prereacted with biotin was also examined in another flow cell of the same chip.

The nonspecific protein adsorption was examined over the PAMAM dendrimer and EO_3-dendrimer layers formed on gold by incubating the dendrimer-modified surface with BSA or serum proteins that had been labeled with fluorescent dyes. FITC-labeled BSA (Sigma) was used after proper dissolution and dilution. Proteins in human serum were labeled with FITC, and FITC-labeled proteins were collected by gel filtration according to the manufacturer's instructions. The dendrimer-layered surfaces were reacted for 1 h with a solution containing the FITC-labeled BSA or human serum protein (1 mg/ml in PBS) and thoroughly rinsed with PBS buffer for a few hours to remove reversibly adsorbed proteins. The water-rinsed and dried gold substrates were fixed onto one side of a glass slide with double-sided tape and mounted on a fluorescent scanner (GenePix 4100A, Axon Instruments Inc., Foster City, CA). The defined area of 4 × 4 mm for each substrate was scanned, and the mean values of fluorescence intensities were determined using the manufacturer's software (Genepix 4.1).

2.5. Procedures for synthesis of an EO_3-dendrimer

The overall procedures for synthesis of an EO_3-dendrimer are presented in Scheme 1. The final product was characterized by ^{1}H and ^{13}C NMR spectroscopy and MALDI-TOF MS.

2.5.1. Synthesis of azido-EO_3-nitrophenyl carbamate (compound 3)

To a solution of azido-EO_3-amine (compound 1, 270 mg, 1.24 mmol) [31,32] and Et_3N (125 mg, 1.24 mmol) in CH_2Cl_2 (10 ml) in an ice bath was added 4-nitrophenyl chloroformate (compound 2, 250 mg, 1.24 mmol), and then the resulting solution was stirred for 2 h in an ice bath and 5 h at room temperature. After the solvent was removed, the residue was purified by column chromatography using EtOAc/*n*-hexane (2:1) as an eluent to afford azido-EO_3-nitrophenyl carbamate (compound 3) at 87% yield. ^{1}H NMR (300 MHz, $CDCl_3$): 3.39 (t, $J = 5.1$ Hz, 2H), 3.49 (t, $J = 5.4$ Hz, 2H), 3.64–3.70 (m, 12H), 5.87 (br s, 1H), 7.33 (d, $J = 9.1$ Hz, 2H), 8.25 (d, $J = 9.1$ Hz, 2H); ^{13}C NMR (125 MHz, $CDCl_3$): 41.6, 51.1, 70.0, 70.5, 70.8, 71.1, 122.4, 125.5, 145.1, 153.7, 156.5; MS (FAB): m/z 354.12 [M^+].

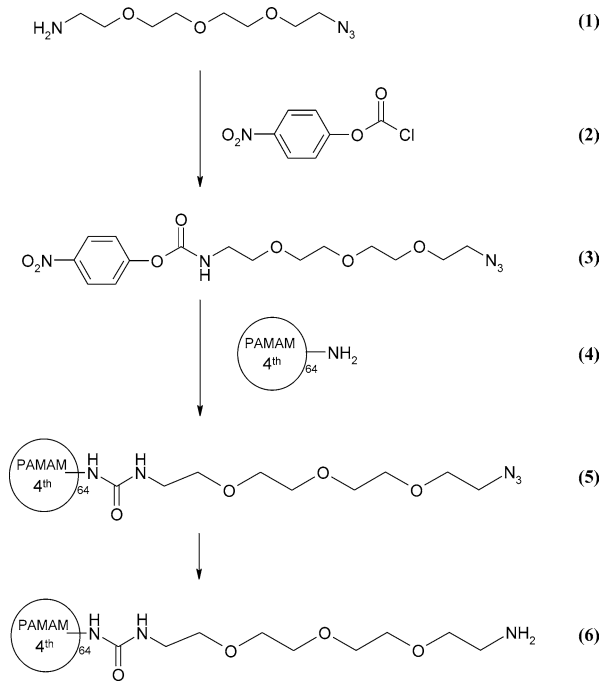

Scheme 1. Overall procedures for synthesis of an EO_3-dendrimer. Azido-EO_3-amine (1) was synthesized according to the known routes [31,32] and reacted with nitrophenyl carbamate (2) to yield azido-EO_3-nitrophenyl carbamate (3). Chemical conjugation between azido-EO_3-nitrophenyl carbamate and G4 PAMAM dendrimer (4) produced the reaction intermediate of azido-EO_3-dendrimer (5), which was further converted to a reduced form of an EO_3-dendrimer (6).

2.5.2. Synthesis of an EO_3-dendrimer (compound 6)

To a solution of a PAMAM dendrimer (compound 4, 40 mg, 2.8 µmol) and Et_3N (28 µl, 0.20 mmol: 1.1 equiv per NH_2 of dendrimer) in DMF (4 ml) in an ice bath was added azido-EO_3-nitrophenyl carbamate (compound 3, 90 mg, 0.24 mmol: 1.3 equiv per NH_2 of dendrimer) and then the resulting solution was stirred for 4 days at room temperature and 1 day at 50 °C. The reaction mixture was concentrated under reduced pressure and the residue was treated with 5% NaOH solution (40 ml) followed by extraction with CH_2Cl_2 (3 × 50 ml). The combined organic solution was washed with a saturated Na_2CO_3 solution (3 × 40 ml), dried, and concentrated to provide the crude compound. This crude azido-EO_3-dendrimer (compound 5) was dissolved in THF (8 ml) and PPh_3 (0.11 g, 0.42 mmol), and H_2O (4 ml) was added. The resulting solution was stirred for 24 h before removal of THF. The solid materials were filtered out and the aqueous solution was dialyzed against distilled water for 48 h using a dialysis bag (molecular weight 3500 cutoff). The lyophilization afforded the EO_3-dendrimer (compound 6, 75 mg). The freshly prepared EO_3-dendrimer was used for further analysis and stored at 4 °C under N_2 gas.

2.5.3. Estimation of a grafting ratio

^{1}H NMR (500 MHz, DMSO-d_6) and ^{13}C NMR (125 MHz, D_2O) were used to determine the grafting ratio

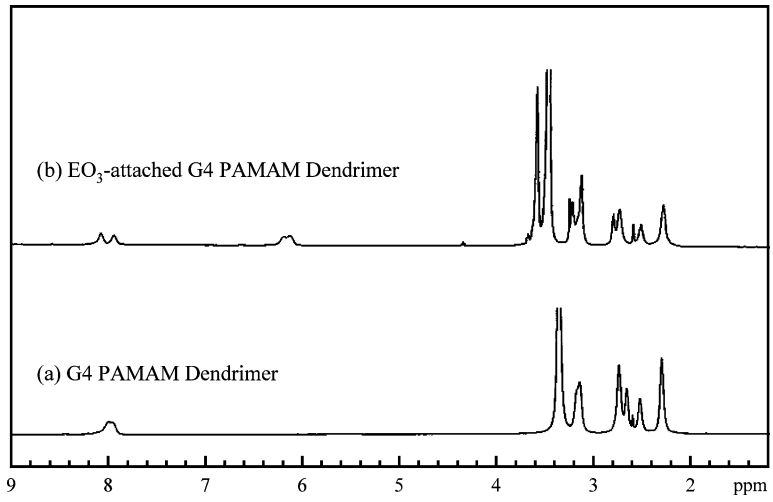

Fig. 1. ^{1}H NMR spectra of a PAMAM dendrimer (a) and EO_3-dendrimer (b).

of the EO_3 unit. ^{1}H NMR (500 MHz, DMSO-$_{d6}$): 2.29 (br, PAMAM unit), 2.52 (br, PAMAM unit), 2.74 (br, PAMAM unit), 2.81 (br, CH_2NH_2 of EO_3 unit), 3.14 (br, PAMAM unit), 3.23 (br, $NHCONHCH_2$ of EO_3 unit), 3.41 and 3.61 (m, $CH_2(OCH_2CH_2O)_3CH_2$ of EO_3 unit), 6.14 and 6.20 (br, –NHCONH–), 7.95 and 8.09 (–CONH–, PAMAM unit); ^{13}C NMR (125 MHz, D_2O): 172.5, 172.2, 159.1, 72.4, 70.9, 70.6, 70.56, 70.4, 70.1, 69.1, 53.0, 50.7, 50.4, 49.5, 41.6, 40.1, 39.9, 37.8, 34.1. The average number of EO_3 units per EO_3-dendrimer was estimated to be 61 (95%) from the integral ratios. MALDI-TOF mass spectra were obtained using Voyager-DE STR biospectrometry (Applied Biosystems, USA) and a 2,5-dihydroxybenzoic acid matrix.

3. Results and discussion

3.1. Synthesis and characterization of the EO_3-dendrimer

In designing a poly(ethylene oxide)-terminated (conjugated) dendrimer, we first determined the chain length of an ethylene oxide unit to be conjugated with the terminal amines of a G4 PAMAM dendrimer by taking into account that the ethylene-oxide-conjugated dendrimer is desired to retain a structural feature of the spherical dendrimer and the resulting layers are resistant to nonspecific protein adsorption. This strategy was reasoned from our and other reports that PAMAM dendrimer monolayers offer efficient protein–ligand interactions [17] and short EO_n-terminated ($n = 3$–6) SAM surfaces are effective in minimizing nonspecific adsorption of various proteins (*vide infra*) [33,34]. Based on these considerations, a tri(ethylene oxide) unit was selected to be attached to a PAMAM dendrimer. The detailed procedures for attachment of EO_3 units to a G4 PAMAM dendrimer were described in Section 2. Briefly, the conjugation reaction was accomplished by adding 1.3 equivalents of the reactive EO_3 unit to 1 equivalent of the terminal amines of a PAMAM dendrimer as shown in Scheme 1. NMR analysis revealed that the EO_3 units were conjugated with the chain ends of a PAMAM dendrimer through urea bonds. Fig. 1 shows the ^{1}H NMR spectra for a G4 PAMAM dendrimer and the synthesized EO_3-dendrimer. It is evident that the spectrum of the EO_3-dendrimer contains signals originating from both G4 PAMAM dendrimer and the EO_3 units. From the integral ratio of the signal at 2.29 ppm, which corresponds to the methylene protons next to the carbonyl groups of the dendrimer, to those at 6.14 and 6.20 ppm, corresponding to the ureic NH protons, the average number of the conjugated EO_3 units in the EO_3-dendrimer was estimated to be 61. This result indicates that more than 95% of the chain-ends of the dendrimer were covalently attached to the EO_3 units.

To further confirm incorporation of EO_3 units, the synthesized EO_3-dendrimer was analyzed using MALDI-TOF MS. A G4 PAMAM dendrimer is monodisperse with a molecular mass of 14,215 Da, and the molecular mass of an EO_3-dendrimer is expected to be around 27,469 Da, given that about 95% of the amine groups of a PAMAM dendrimer are conjugated with EO_3 units. As shown in Fig. 2, a mass peak of $\sim$27,500 amu was distinctly observed, which is consistent with the results from the NMR analysis. The PAMAM dendrimer generated a peak centered at 14,215 amu. As recently observed by Baker et al. [35], a series of peaks at lower m/z were found in mass spectra for both molecules. They seem to be generated by fragmentation of the molecules during ionization, based on the observation that a mass peak of around 27,500 amu can be derived from the EO_3-dendrimer.

3.2. Surface characterization of the EO_3-dendrimer layers on gold

To investigate the surface characteristics of the EO_3-dendrimer layers, we constructed the layers of EO_3-dendrimers on reactive SAMs on gold as described in Section 2. IR-RA spectroscopy was employed to verify the coupling reaction of PAMAM dendrimers or EO_3-dendrimers with the N-hydroxysuccinimide activated 11-mercaptoundecanoic

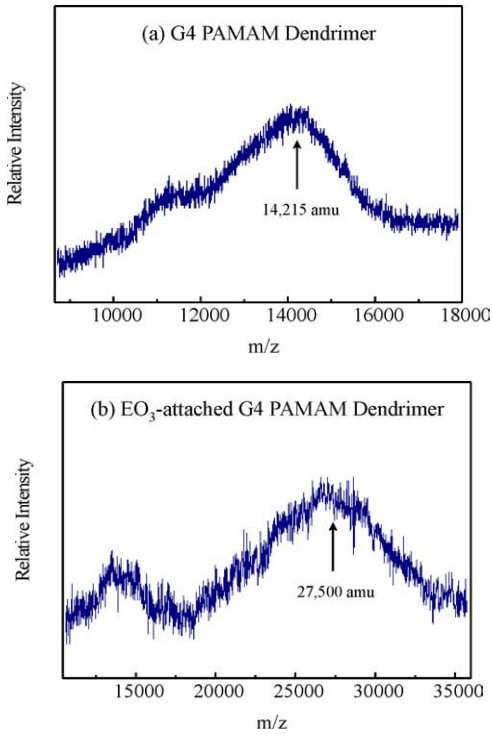

Fig. 2. MALDI-TOF mass spectra of a PAMAM dendrimer (a) and EO_3-dendrimer (b).

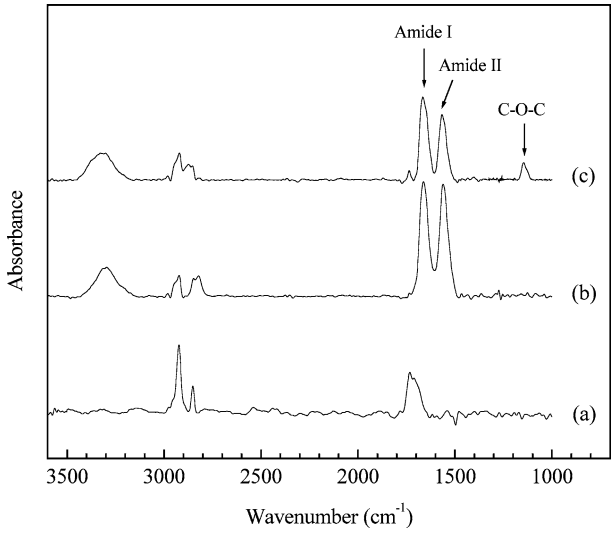

Fig. 3. IR-RA spectra of the MUA SAM surface on gold (a); PAMAM dendrimer monolayers on MUA SAMs/Au (b); EO_3-dendrimer layers on MUA SAMs/Au (c).

acid (MUA) SAMs on gold. The spectra for MUA SAMs on gold exhibited asymmetric and symmetric CH_2 bands at 2923 and 2851 cm^{-1} and a COOH band at 1724 cm^{-1} (Fig. 3a), which are consistent with the reports of the Crooks group [3–6]. The amide I and II bands at 1660 and 1559 cm^{-1} in Figs. 3b and 3c confirmed that the dendrimers were amide-coupled to the underlying activated MUA SAMs. The additional bands at 2920–2820 cm^{-1} resulted from the two kinds of methylene groups, and the amide and amine N–H stretching modes centered around 3300 cm^{-1} also appeared in both PAMAM dendrimer and EO_3-dendrimer layers. In contrast, only EO_3-dendrimer layers on MUA SAMs/Au generated the C–O–C band at 1143 cm^{-1}, indicating coexistence of EO_3 units in the dendrimer-immobilized surface.

Table 1
Ellipsometric thicknesses and contact angles

Modified surfaces	Ellipsometric thickness (Å)	Contact angle (°)
None (bare Au)	–	66 ± 2
MUA SAMs/Au	16 ± 2	27 ± 3
G4 PAMAM dendrimer monolayers[a]	28 ± 3	31 ± 1
EO_3-dendrimer layers[a]	24 ± 2	26 ± 2

[a] PAMAM dendrimer and EO_3-dendrimer layers were constructed over the SAMs of MUA on gold.

Ellipsometric thicknesses for both layers are shown in Table 1. The thickness of MUA SAMs on gold was 16 ± 2 Å, which closely matches the reported values [36,37]. The thicknesses of the PAMAM dendrimer and EO_3-dendrimer layers excluding MUA SAMs on gold were estimated to be 28 ± 3 and 24 ± 2 Å, respectively. More than five different points of the same substrate were measured and a layering process with the EO_3-dendrimer was prolonged for more than 5 h. Estimated values were within experimental error. Especially, almost identical results were obtained regardless of the layer-forming conditions (either in a methanolic or in an aqueous solution). Afterward, we prepared the EO_3-dendrimer layers in an aqueous phase to elicit the proper conformation of the EO_3 chains in the resulting layers. It is well known that the thickness of PAMAM dendrimer monolayers decreases markedly mainly due to substantial distortion of the dendrimer when it is immobilized and confined on a flat surface. We and the Crooks group reported that the monolayers of PAMAM dendrimers have a thickness of about 26 ± 2 Å, showing a much smaller value than the bulk dimension of the dendrimer (45 Å) [5,17]. Unexpectedly, the EO_3-dendrimer resulted in layers with a measured thickness of 24 ± 2 Å, slightly thinner than the PAMAM dendrimer monolayers, which indicates that the effect of the conjugated EO_3 units on the layer thickness was negligible. The bulk dimension of the EO_3-dendrimer is estimated to be around 80 Å by Insight II software. Considering this, the measured thickness of the EO_3-dendrimer layers is much smaller than expected, which implies that the layer-forming process for the EO_3-dendrimer may be different from that for the PAMAM dendrimers. This presumption might be supported by the IR-RA spectra shown in Figs. 3b and 3c. The relative peak intensity of the amide I and II bands in the PAMAM dendrimer monolayers was 1.7-fold greater than that in the EO_3-dendrimer layers. It has been observed that PAMAM dendrimers are closely packed with a substantial distortion when covalently attached to the activated MUA SAMs [5,17,38]. Through the electrochemical titra-

tion of ferrocene-modified dendrimer monolayers, we and the Crooks group demonstrated that the dendrimer coverage corresponds to nearly 270–280% of a theoretical estimate from its bulk dimension. Based on the results from ellipsometry and IR-RA studies, we conclude that no significant deformation of the EO_3-dendrimer occurred during its immobilization onto MUA SAMs and relatively less compact layers were formed than by PAMAM dendrimers.

The entirely different phenomenon in the formation of the EO_3-dendrimer layers might be caused by a steric repulsion effect derived from the fully attached EO_3 chains having a brushlike conformation [39]. Generally known is that the steric repulsion mechanism induces a poly(ethylene oxide)-containing molecule to self-exclude during preparation of its layers on a solid surface [40–43]. This effect of the poly(ethylene oxide) chains was definitely demonstrated by the experimental observation that as two poly(ethylene oxide)-coated surfaces approach each other, the repulsive force between them develops at a certain separation distance [40]. Similarly, in the process of layer-formation by the EO_3-dendrimer, close approach of the EO_3-dendrimer to the preoccupied molecules on a flat surface can be hindered due to intermolecular repulsion, which affects the packing density of the EO_3-dendrimer in the resulting layers.

Nonetheless, the formation of uniform layers by the EO_3-dendrimer was confirmed from the IR-RA and ellipsometric analyses. Accordingly, the height of the EO_3-dendrimer layers might be more significantly reduced than that of the PAMAM dendrimer monolayers during drying with N_2 gas, which resulted in a smaller thickness of 24 ± 2 Å. A similar result was reported by Emmrich et al. [7]. A thiol-terminated G4 PAMAM dendrimer with a diameter of about 70–80 Å lost up to 70% of its height due to the loss of solvent, when deposited on a surface and dried; consequently, the thickness of the resulting layers was about 25 Å.

The contact angle of the EO_3-dendrimer layers was measured and compared with those of other layers (Table 1). The contact angles of a cleaned gold surface, a MUA SAM surface, and PAMAM dendrimer layers were $66 \pm 2°$, $27 \pm 3°$, and $31 \pm 1°$, respectively, as reported elsewhere [5,44]. The EO_3-dendrimer layers were found to have a smaller contact angle ($26 \pm 2°$) than the PAMAM dendrimer layers, probably due to incorporation of EO_3 units and less compactness of the layers.

3.3. Avidin–biotin interaction and protein adsorption tests

As an interface for bioaffinity sensing, we tested whether the EO_3-dendrimer layers retain the innate properties of PAMAM dendrimer monolayers for avidin–biotin interactions. In our previous work, we observed that the surface coverage by avidin on the biotinylated dendrimer monolayers on gold reaches about 88% of full coverage [17], showing a much higher value than a SAM-based surface (41%) or poly-L-lysine layer (56%). This observation seemed to be attributable to the unique structural features of PAMAM

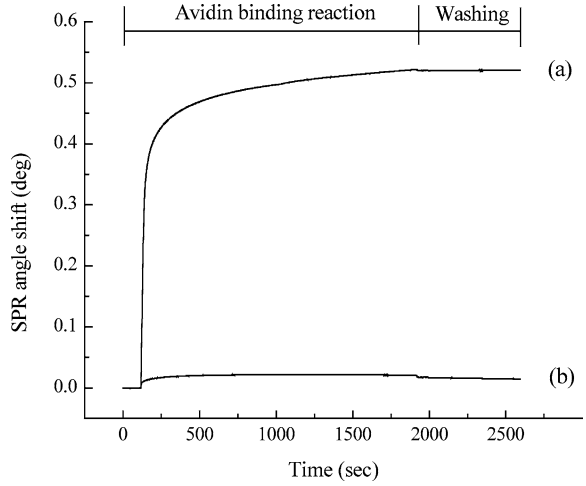

Fig. 4. SPR sensorgram for specific binding (a) and nonspecific adsorption of avidin (b) over the EO_3-dendrimer layers that had been biotinylated with a sulfo-NHS-biotin reagent (2 mg/ml). The avidin sample (50 μg/ml in PBS) was injected for 30 min at a flow rate of 3 μl/min. Nonspecific binding of avidin was also measured by treating the biotinylated surface with avidin prereacted with free biotin. The change in a SPR response was recorded after a proper washing with PBS buffer.

dendrimer monolayers, such as a corrugated surface and surface exposure of functionalized biotin ligands. We reasoned that the EO_3-dendrimer layers can also have a property comparable to that of the dendrimer monolayers in achieving a substantially high level for avidin binding. As shown in an SPR sensorgram of Fig. 4, an avidin binding reaction was performed at the EO_3-dendrimer layer that had been biotinylated with a sulfo-NHS-biotin reagent of 1 mg/ml (∼2 mM final concentration). The amount of bound avidin reached the surface density of about 5.2 ± 0.2 ng mm^{-2}, corresponding to about 92% of full surface coverage. As stated earlier, the EO_3-dendrimers resulted in less compact layers, but interestingly an association level of avidin similar to that of the PAMAM dendrimer monolayers was obtained. Our previous study explained in detail the avidin association level with respect to the surface density of biotin ligands. Compared with other layers tested, including mixed SAMs and poly-L-lysine layers, the biotinylated PAMAM dendrimer monolayers showed higher association levels of avidin over a broad range of biotin concentrations. In other words, the association level of avidin reached a maximum at a low concentration of biotin ligands and maintained a substantially high coverage even up to high biotin concentrations. This result seemed to be due to surface exposure of derivatized biotin ligands and a corrugated surface structure. In this regard, the comparability of the avidin coverage at the less compact EO_3-dendrimer layers to that for the PAMAM dendrimer monolayers might also be explained by the structural features of the EO_3-dendrimer layers. The extent of nonspecific avidin binding was estimated to be <0.2 ng mm^{-2} when avidin preblocked with free biotin was reacted. Favorably affected by the introduction of EO_3 units, nonspecific adsorption of avidin in the present system was considerably

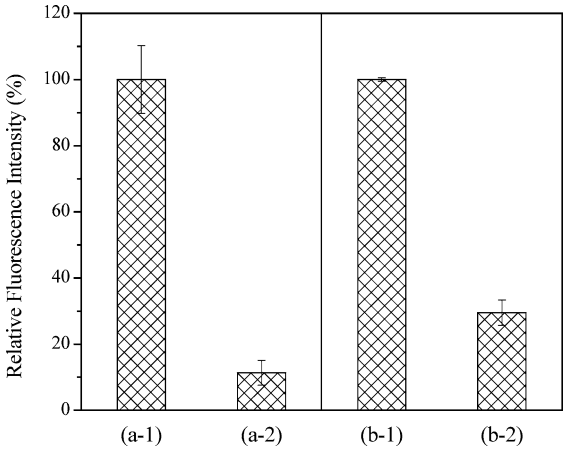

Fig. 5. Nonspecific binding of BSA (1 mg/ml in PBS) labeled with FITC over the PAMAM dendrimer (a-1) and EO_3-dendrimer layers (a-2); nonspecific adsorption of serum proteins (1 mg/ml in PBS) labeled with FITC over the PAMAM dendrimer (b-1) and EO_3-dendrimer layers (b-2).

reduced to a level threefold lower than that of the PAMAM dendrimer layers.

To compare the effectiveness of dendrimer-modified surfaces in reducing the nonspecific protein adsorption, fluorescent intensities resulting from adsorbed proteins were measured after treatment of FITC-labeled protein samples for 1 h and extensive washing with fresh PBS buffer. As shown in Fig. 5, the EO_3-dendrimer layers were more resistant to adsorption of BSA and serum proteins than the PAMAM dendrimer layers. The extent of nonspecific adsorption of BSA and serum proteins was about 11.4 and 29.5% of those on the PAMAM dendrimer layers, respectively. It was reported that short EO_n ($n = 3$–6) units are effective in preventing nonspecific adsorption of various proteins and serum-containing media [33,34]. On the other hand, the EO_3-dendrimer layers were found to be less resistant to adsorption of serum proteins, two major constituents of which are albumin and fibrinogen, than expected. This illustrates that the EO_3-dendrimer layers did not play a role in minimization of nonspecific protein adsorption as much as the ethylene-oxide-incorporated SAM surface [33,45]. It was suggested that the surfaces resistant to protein adsorption possess an overall neutral charge and terminal groups that are hydrophilic and function as hydrogen bond acceptors [45]. On the contrary to these requirements, the terminal amines of the EO_3-dendrimer layers would be positively charged under the reaction condition of pH 7.4, hence acting as a hydrogen bond donor, which is attributed to diminished resistance of the EO_3-dendrimer layers to protein adsorption. This explanation might be supported from the result by Chirakul et al. regarding the nonspecific adsorption of proteins onto the amine-terminated SAM surface [46]. They prepared and surface characterized the mixed SAMs consisting of di(ethylene glycol)-terminated thiolates and amine-terminated, di(ethylene glycol)-incorporated thiolates, preferable to covalent coupling of a wide variety of biomolecules. The amine-terminated SAM surface was slightly effective in preventing nonspecific adsorption of BSA, but not for fibrinogen. This trend is similar to our observations, but the SAMs of amine-terminated, di(ethylene glycol)-incorporated thiolates appear to be less resistant to nonspecific adsorption of BSA compared to the EO_3-dendrimer layers. The EO_3-dendrimer layers could not afford to fully minimize nonspecific adsorption of proteins, but our results demonstrate that the EO_3-conjugated PAMAM dendrimers render the surface more effective in reducing the nonspecific adsorption of proteins than the PAMAM dendrimers.

4. Conclusion

This paper demonstrated that the conjugation of EO_3 units with terminal amines of a G4 PAMAM dendrimer renders its layered surface more resistant to adsorption of proteins, while retaining an avidin–biotin interaction efficiency similar to that of the G4 PAMAM dendrimer monolayers. NMR and MALDI-TOF MS analyses revealed that about 95% of the chain-ends of a PAMAM dendrimer are covalently attached to the EO_3 units. The surface characterization by IR-RA spectroscopy, ellipsometry, and contact angle goniometry indicated that the EO_3-dendrimer also generated uniform and more hydrophilic layers on gold, compared to the PAMAM dendrimer monolayers. The surface density of avidin on the biotinylated EO_3-dendrimer layers was estimated to be 5.2 ± 0.2 ng mm^{-2}, which corresponds to about 92% of full surface coverage. The EO_3-dendrimer layers were observed to be considerably effective in lowering nonspecific adsorption of BSA, but exhibited a slightly increased resistance to adsorption of serum proteins, compared to the PAMAM dendrimer monolayers.

Acknowledgments

This work was supported by the BK21 Program of the Korean Ministry of Education and by the National Research Laboratory Program (H.S. Kim) and the Creative Research Initiative Program (K. Kim) of the Korean Ministry of Science and Technology. We thank Professor Insung S. Choi and Young-Shik Chi (Department of Chemistry, KAIST) for technical assistance.

References

[1] J.M.J. Fréchet, Proc. Natl. Acad. Sci. U.S.A. 99 (2002) 4782.
[2] D.C. Tully, J.M.J. Fréchet, Chem. Commun. 14 (2001) 1229.
[3] M. Wells, R.M. Crooks, J. Am. Chem. Soc. 118 (1996) 3988.
[4] H. Tokuhisa, R.M. Crooks, Langmuir 13 (1997) 5608.
[5] H. Tokuhisa, M. Zhao, L.A. Baker, V.T. Phan, D.L. Dermody, M.E. Garcia, R.F. Peez, R.M. Crooks, T.M. Mayer, J. Am. Chem. Soc. 120 (1998) 4492.
[6] V. Chechik, R.M. Crooks, Langmuir 15 (1999) 6394.

[7] E. Emmrich, S. Franzka, G. Schmid, J.-P. Majoral, Nano Lett. 2 (2002) 1239.
[8] G. Bar, S. Rubin, R.W. Cutts, T.N. Taylor, T.A. Zawodzinski, Langmuir 12 (1996) 1172.
[9] Y. Liu, M.L. Bruening, D.E. Bergbreiter, R.M. Crooks, Angew. Chem. Int. Ed. Engl. 36 (1997) 2114.
[10] D.C. Tully, K. Wilder, J.M.J. Fréchet, A.R. Trimble, C.F. Quate, Adv. Mater. 11 (1999) 314.
[11] R. McKendry, W.T.S. Huck, B. Weeks, M. Fiorini, C. Abell, T. Rayment, Nano Lett. 2 (2002) 713.
[12] R. Benters, C.M. Niemeyer, D. Wöhrle, Chem. Bio. Chem. 2 (2001) 686.
[13] A.-C. Chang, J.B. Gillespie, M.B. Tabacco, Anal. Chem. 73 (2001) 467.
[14] L. Svobodová, M. Šnejdárková, T. Hianik, Anal. Bioanal. Chem. 373 (2002) 735.
[15] N. Krasteva, I. Besnard, B. Guse, R.E. Bauer, K. Mullen, A. Yasuda, T. Vossmeyer, Nano Lett. 2 (2002) 551.
[16] H.C. Yoon, D. Lee, H.-S. Kim, Anal. Chim. Acta 456 (2002) 209.
[17] M.-Y. Hong, H.C. Yoon, H.-S. Kim, Langmuir 19 (2003) 416.
[18] M. Mrksich, G.M. Whitesides, ACS Symp. Ser. 680 (1997) 361.
[19] R.G. Chapman, E. Ostuni, L. Yan, G.M. Whitesides, Langmuir 16 (2000) 6927.
[20] M. Riepl, K. Enander, B. Liedberg, M. Schäferling, M. Kruschina, F. Ortigao, Langmuir 18 (2002) 7016.
[21] N. Xia, Y. Hu, D.W. Grainger, D.G. Castner, Langmuir 18 (2002) 3255.
[22] N.-P. Huangs, J. Vörös, S.M. De Paul, M. Textor, N.D. Spencer, Langmuir 18 (2002) 220.
[23] S. Herrwerth, T. Rosendahl, C. Feng, J. Fick, W. Eck, M. Himmelhaus, R. Dahint, M. Grunze, Langmuir 19 (2003) 1880.
[24] K.L. Prime, G.M. Whitesides, Science 252 (1991) 1164.
[25] J.M. Harris, Poly(ethylene glycol) Chemistry, Plenum, New York, 1992.
[26] S.I. Jeon, J.D. Andrade, J. Colloid Interface Sci. 142 (1991) 159.
[27] D. Luo, K. Haverstick, N. Belcheva, E. Han, W.M. Saltzman, Macromolecules 35 (2002) 3456.
[28] C. Kojima, K. Kono, K. Maruyama, T. Takagishi, Bioconjugate Chem. 11 (2000) 910.
[29] R.C. Hedden, B.J. Bauer, A.P. Smith, F. Gröhn, E. Amis, Polymer 43 (2002) 5473.
[30] R.C. Hedden, B.J. Bauer, Macromolecules 36 (2003) 1829.
[31] A.W. Schwabacher, J.W. Lane, M.W. Schiesher, K.M. Leigh, C.W. Johnson, J. Org. Chem. 63 (1998) 1727.
[32] J.W. Lee, P.L. Fuchs, Org. Lett. 1 (1999) 179.
[33] K.L. Prime, G.M. Whitesides, J. Am. Chem. Soc. 115 (1993) 10714.
[34] B. Zhu, T. Eurell, R. Gunawan, D. Leckband, J. Biomed. Mater. Res. 56 (2001) 406.
[35] W.S. Baker, B.I. Lemon, R.M. Crooks, J. Phys. Chem. B 105 (2001) 8885.
[36] R.C. Sabapathy, R.M. Crooks, Langmuir 16 (2000) 7783.
[37] J.C. Love, D.B. Wolfe, R. Haasch, M.L. Chabinyc, K.E. Paul, G.M. Whitesides, R.G. Nuzzo, J. Am. Chem. Soc. 125 (2003) 2597.
[38] H.C. Yoon, M.-Y. Hong, H.-S. Kim, Anal. Chem. 72 (2000) 4420.
[39] Z. Yang, J.A. Galloway, H. Yu, Langmuir 15 (1999) 8405.
[40] J. Klein, P. Luckham, Nature 300 (1982) 429.
[41] M. Malmsten, Biopolymers at Interfaces, Dekker, New York, 1998.
[42] S.I. Jeon, J.H. Lee, J.D. Andrade, P.G. de Gennes, J. Colloid Interface Sci. 142 (1991) 149.
[43] K. Bergstrom, E. Osterberg, K. Holmberg, A.S. Hoffman, T.P. Schuman, A. Kozlowski, J.M. Harris, J. Biomater. Sci. Polym. Ed. 6 (1994) 123.
[44] N. Patel, M.C. Davies, M. Hartshorne, R.J. Heaton, C.J. Roberts, S.J.B. Tendler, P.M. Williams, Langmuir 13 (1997) 6485.
[45] E. Ostuni, R.G. Chapman, R.E. Holmlin, S. Takayama, G.M. Whitesides, Langmuir 17 (2001) 5605.
[46] P. Chirakul, V.H. Pérez-Luna, H. Owen, G.P. López, P.D. Hampton, Langmuir 18 (2002) 4324.